Article Info

Soret and Dufour Effects on an Unsteady MHD Flow through Porous Medium with Hall Current

Mohammad Faisal Khan*, Abdulaziz Alorainni** and Rajeev Jha***

ABSTRACT

Aim of this paper to investigate Soret (thermal-diffusion) and Dufour (diffusion-thermo) effects on unsteady MHD flow through porous medium in the presence of a magnetic field with hall current. The similarity solutions were obtained using suitable transformations and the resulting similarity ordinary differential equations were solved by finite difference method. The influences of different flow parameters on velocity, temperature and concentration fields are investigated. The skin frictions at the plate due to tangential and lateral velocity fields are obtained in non-dimensional form. The effects of the physical parameters like Dufour number (Du) and Soret number (Sr) on these fields are discussed through graphs and results are physically interpreted.

Keywords: MHD; Porous Medium; Heat Transfer; Mass Transfer; Soret Number; Dufour Number; Hall Current; Porous Flat Plate; Finite Difference Method.

1.0 Introduction

The ranges of free convective flows that occur in nature and in engineering practice is very large and have been extensively considered by many researchers. When heat and mass transfer occur simultaneously between the fluxes, the driving potentials are of more intricate nature. An energy flux can be generated not only by temperature gradients but also by composition gradients as well. The energy flux caused by a composition gradient is called Dufour or Diffusion-thermo effect. Temperature gradients can also create mass fluxes, and this is the Soret or thermal-diffusion effect. Generally, the thermal-diffusion and the diffusion-thermo effects are of smaller-order magnitude than the effects prescribed by Fourier's or incompressible, electrically conducting fluid over a stretching sheet in the presence of suction and injection with thermal diffusion and diffusion-thermo effects. Alam et al. [3] studied numerically the Dufour and Soret effects on combined free-forced convection and mass transfer flow past a semi-infinite vertical plate under the influence of transversely applied magnetic field. Ambethkar [4] investigated numerical solutions of heat and mass transfer effects of an unsteady MHD free convective flow past an infinite vertical plate with constant suction. Chin et al. [5] obtained numerical results for the steady mixed convection boundary layer flow over a vertical impermeable surface embedded in a porous medium when the viscosity of the fluid varies inversely as a linear function of the temperature. Gaikward et al. [6] investigated the onset of double diffusive convection in two component couple of stress fluid layer with Soret and Duffour effects using both linear and non-linear stability analysis. Hayat et al. [7] discussed the effects of Soret and Dufour on heat and mass transfer on mixed convection boundary layer flow over a stretching vertical surface in a porous medium filled with a viscoelastic fluid. Kafoussias et al. [8] considered the boundry layer – flows in the presence of Soret, and Dufour effects associated with the thermal diffusion and diffusion thermo for the mixed forced natural convection. Lyubinova et al. [9] deals with the numerical investigation of the influence of static and vibrational acceleration on the measurement of diffusion and Sorect coefficients in binary mixtures, in low gravity conditions. Mansour et al. [10] investigated the effects of chemical

*College of Science & Theoretical Studies, Saudi Electronic University, Riyadh KSA

**College of Engineering, Teerthanker Mahaveer University, Moradabad, India

**Corresponding Author: College of Engineering, Teerthanker Mahaveer University, Moradabad, India

(E-mail: jhadrrajeev@gmail.com)

reaction, thermal stratification, Soret and Dufour numbers on MHD free convective heat and mass transfer of viscous, incompressible and electrically conducting fluid over a vertical stretching surface embedded in a saturated porous medium.

Ming-chun et al. [11] studied Soret and Dufour effects in strongly endothermic chemical reaction system of porous media. Motsa [12] investigated the effects of Soret and Dufour numbers on the onset of double diffusive convection.

Mukhopadhyay [13] performed an analysis to investigate the effects of thermal radiation on an unsteady mixed convection flow and heat transfer over a porous stretching surface in porous medium. Osalusi et al. [14] investigated thermo-diffusion and diffusion – thermo effects on combined heat and mass transfer of a steady hydro magnetic convective and slip flow due to a rotating disk in the presence of viscous dissipation and ohmic heating.

Pal et al. [15] analyzed the combined effects of mixed convection with thermal radiation and chemical reaction of MHD flow of viscous and electrically conducting fluid past a vertical permeable surface embedded in a porous medium. Shateyi [16] investigated thermal radiation and buoyancy effects on heat and mass transfer over a semi-infinite stretching surface with suction and blowing. Srihari et al. [17] discussed Soret effect on unsteady MHD free convective mass transfer flow past an infinite vertical porous plate with oscillatory suction velocity and heat sink. More recently Vempati et al.

[18] studied numerically the effects of Dufour and Soret numbers Fick's laws and are often neglected in heat and mass transfer processes. However, there are exceptions.

The thermal-diffusion effect, for instance, has been utilized for isotope separation and in mixture between gases with very light molecular weight (Hydrogen – Helium) and of medium molecular weight (Nitrogen – Air) the diffusion thermo effect was found to be of a magnitude such that it cannot be neglected (see Kafoussias et al. [18] and reference therein).

In recent years, progress has been considerably made in the study of heat and mass transfer through porous media in magnetohydro dynamic flows due to its application in many devices.

The effect of hall currents on the fluid has a lot of applications in MHD power generators, several astrophysical and meteorological studies as well as in flow of plasma through MHD power generators.

From the point of applications, this effect can be taken into account within the range of magnetohydrodynamical approximation.

Abreu et al. [1] examined the boundary layer solutions for the cases of forced, natural and mixed convection under a continuous set of similarity type of variables determined by a combination of pertinent variables measuring the relative importance of buoyancy force term in the momentum equation. Afify [2] carried out an analysis to study free convective heat and mass transfer of an on an unsteady MHD flow past an infinite vertical porous plate with thermal radiation. Vempati et al.

[18] have studies on Soret and Dufour effects on unsteady MHD flow past an infinite vertical porous plate with thermal radiation. Recently, Rao and Raju [19] have discussed on the effect of hall currents, Soret and Dufour on an unsteady MHD flow and heat transfer along a porous flat plate with mass transfer.

Motivated by the above reference work and the numerous possible industrial application of the problem (like in isotope separation), it is of paramount interest in this study to investigate the Soret and Dufour effects on MHD flow through porous medium along a porous flat plate.

Hence, the purpose of this paper is to extend the results of Rao and Raju [19] to study the more general problem which includes the Soret and Dufour effects on an unsteady MHD flow through porous medium and heat transfer along a porous flat plate in presence of hall currents. In this study, the effects of different flow parameters encountered in the equations are also studied. The problem is solved numerically using the finite difference method, which is more economical from the computational view point.

2.0 Mathematical Analysis

We choose $x'-$ axis along the plate in direction and $y'-$ axis is normal to it. Initially, the temperature of the plate and the fluid through porous medium is assumed to be same. At time $t' > 0,$ the plate starts moving with a velocity in its own plane and its temperature is instantaneously raised or lowered to T which is thereafter maintained constant. Since the plate is infinite Ct' in length, all physical quantities are functions of y' and t' only. Hence, if the velocity V' is given by

(u', v', w'), the equation of continuity, on integration gives

$$v_0' = \text{constant} = -V_0'(say);$$

Where v_0' is the constant normal velocity of suction or injection at the plate according to $v_0' > 0$ or < 0 respectively. Again if $\overline{H} = (H_x, H_y, H_z)$, the divergence equation of the magnetic field give $H_y = $ constant $= H_0$ (say); Where H_0 is the externally applied transverse magnetic field. Using the relation $\nabla \cdot \overline{J} = 0$ for the current density $\overline{J} = (J_x, J_y, J_z)$, we get $J_y = $ constant. Since the plate is non-conducting $J_y = 0$ at the plate and hence zero everywhere. The magnetic Reynolds number of the flow is taken to be small enough so that the induced magnetic field can be neglected. When the strength of magnetic field is very large the generalized Ohm's law in the absence of electric field takes the following form:

$$\overline{J} + \frac{\omega_e \tau_e}{B_o} \overline{J} \times \overline{H} = \sigma \left(\mu_e \overline{V} \times \overline{H} + \frac{1}{e n_e} \nabla P_e \right) \quad (1)$$

Fig. A: The Coordinate System for the Physical Model Of The Problem.
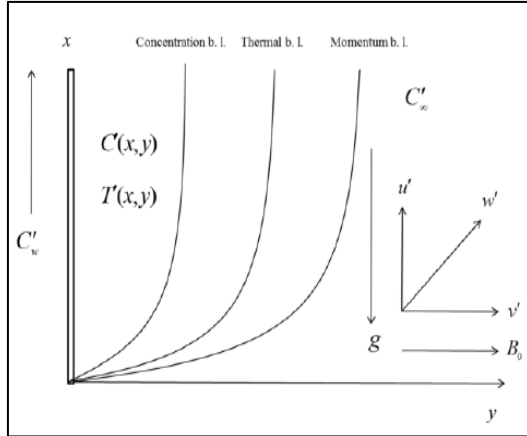
Under the assumption that the electron pressure (for weakly ionized gas), the thermo-electric pressure and ion-slip are negligible, equation (1) becomes.

$$J_x = \frac{\sigma \mu_e H_o}{1+m^2}(mu' - w') \text{ and } J_z = \frac{\sigma \mu_e H_o}{1+m^2}(mw' + u') \quad (2)$$

Where u' is the x - component of $\overline{V}$, w' is the z-component of $\overline{V}$ and m $(= \omega_e \tau_e)$ is the Hall numbers within the above framework, the equations which govern the flow under the usual Boussinesq's approximation are as follows:

$$\frac{\partial v'}{\partial y'} = 0 \quad (3)$$

$$\frac{\partial u'}{\partial t'} + v_0' \frac{\partial u'}{\partial y'} = \upsilon \frac{\partial^2 u'}{\partial y'^2} + g\beta(T' - T_\infty') + g\beta^*(C' - C_\infty')$$

$$- \frac{\sigma \mu_e^2 H_0^2}{\rho(1+m^2)}(u' + mw') - \frac{\upsilon}{K'}u' \quad \ldots(4)$$

$$\frac{\partial w'}{\partial t'} + v_0' \frac{\partial w'}{\partial y'} = \upsilon \frac{\partial^2 w'}{\partial y'^2} - \frac{\sigma \mu_e^2 H_0^2}{\rho(1+m^2)}(w' - mu') - \frac{\upsilon}{K'}w' \quad (5)$$

$$\frac{\partial T'}{\partial t'} + v_0' \frac{\partial T'}{\partial y'} = \frac{k}{\rho c_p}\frac{\partial^2 T'}{\partial y'^2} + \frac{D_m k_T}{c_s c_p}\frac{\partial^2 C'}{\partial y'^2} \quad (6)$$

$$\frac{\partial C'}{\partial t'} + v_0' \frac{\partial C'}{\partial y'} = D\frac{\partial^2 C'}{\partial y'^2} + \frac{D_m k_T}{T_m}\frac{\partial^2 T'}{\partial y'^2} \quad (7)$$

In equation (6) the term due to viscous dissipation is neglected and in equation (7) the term due to chemical reaction is assumed to be absent. The initial and boundary conditions of the problem are:

$$\left. \begin{array}{l} t' \le 0: u' = 0, \ w' = 0, \ T' = T_\infty', \ C' = C_\infty' \quad \text{for all } y' \\ t' > 0: u' = Ut', \ w' = 0, \ T' = T_w', \ C' = C_w' \quad \text{at } y' = 0 \\ u' = 0, \ w' = 0, \ T' = T_\infty', \ C' = C_\infty' \quad \text{as } y' \to \infty \end{array} \right\} \quad (8)$$

The non-dimensional quantities introduced in the equations (3) – (7) are:

$$\left. \begin{array}{l} t = t'\left(\frac{c^2}{\upsilon}\right)^{1/3}, \quad y = y'\left(\frac{c}{\upsilon^2}\right)^{1/3}, \quad (u,v,w) = \frac{(u', v_0', w')}{(\upsilon c)^{1/3}} \\ \theta = \frac{(T' - T_\infty')}{(T_w' - T_\infty')}, \quad C = \frac{(C' - C_\infty')}{(C_w' - C_\infty')}, \quad M = \frac{\sigma \mu_e^2 H_0^2 \upsilon^{1/3}}{\rho c^{2/3}} \\ \Pr = \frac{\mu c_p}{k_T}, \quad Sc = \frac{\upsilon}{D}, \quad Gr = \frac{\upsilon g\beta(T_w' - T_\infty')}{U^3}, \\ Gm = \frac{\upsilon g\beta^*(C_w' - C_\infty')}{U^3}, \quad Du = \frac{D_m k_T(C_w' - C_\infty')}{\upsilon c_s c_p(T_w' - T_\infty')}, \\ Sr = \frac{D_m k_T(T_w' - T_\infty')}{\upsilon T_m(C_w' - C_\infty')}, \quad K = \frac{c^{2/3} K'}{\upsilon^{5/3}} \end{array} \right\} \quad (9)$$

Where U is the reference velocity. The governing equations can be obtained in the dimension less form as:

$$\frac{\partial v}{\partial y} = 0 \quad (10)$$

$$\frac{\partial u}{\partial t} + v\frac{\partial u}{\partial y} = \frac{\partial^2 u}{\partial y^2} + Gr\theta + Gm\phi - \frac{M}{(1+m^2)}(u + mw) - \frac{1}{K}u \quad (11)$$

$$\frac{\partial w}{\partial t} + v\frac{\partial w}{\partial y} = \frac{\partial^2 w}{\partial y^2} - \frac{M}{(1+m^2)}(w - mu) - \frac{1}{K}w \quad (12)$$

$$\frac{\partial \theta}{\partial t} + v\frac{\partial \theta}{\partial y} = \frac{1}{\Pr}\frac{\partial^2 \theta}{\partial y^2} + (Du)\left(\frac{\partial^2 \phi}{\partial y^2}\right) \quad (13)$$

$$\frac{\partial \phi}{\partial t} + v\frac{\partial \phi}{\partial y} = \frac{1}{Sc}\frac{\partial^2 \phi}{\partial y^2} + (Sr)\left(\frac{\partial^2 \theta}{\partial y^2}\right) \quad (14)$$

And the boundary conditions (8) in the non-dimensional form are:

$$t \leq 0: u = 0, \quad w = 0, \quad \theta = 0, \quad \phi = 0 \quad for \ all \quad y$$

$$t > 0: u = 1, \quad w = 0, \quad \theta = 1, \quad \phi = 1 \quad at \quad y = 0$$

$$u = 0, \quad w = 0, \quad \theta = 0, \quad \phi = 0 \quad as \quad y \rightarrow \infty \quad (15)$$

From equation (10), we see the v is either constant or a function of time t.

$$\left[\frac{u_{i,j+1} - u_{i,j}}{\Delta t}\right] + v_{i,j}\left[\frac{u_{i+1,j} - u_{i,j}}{\Delta y}\right] = \left[\frac{u_{i+1,j} - 2u_{i,j} + u_{i-1,j}}{(\Delta y)^2}\right] + Gr\theta_{i,j} + Gm\phi_{i,j}$$

$$- \frac{M}{(1+m^2)}\left(u_{i,j} + mw_{i,j}\right) - \frac{1}{K}u_{i,j} \quad ...(16)$$

$$\left[\frac{w_{i,j+1} - w_{i,j}}{\Delta t}\right] + v_{i,j}\left[\frac{w_{i+1,j} - w_{i,j}}{\Delta y}\right] = \left[\frac{w_{i+1,j} - 2w_{i,j} + w_{i-1,j}}{(\Delta y)^2}\right]$$

$$- \frac{M}{(1+m^2)}\left(w_{i,j} - mu_{i,j}\right) - \frac{1}{K}w_{i,j} \quad ...(17)$$

$$\left[\frac{\theta_{i,j+1} - \theta_{i,j}}{\Delta t}\right] + v_{i,j}\left[\frac{\theta_{i+1,j} - \theta_{i,j}}{\Delta y}\right] = \frac{1}{Pr}\left[\frac{\theta_{i+1,j} - 2\theta_{i,j} + \theta_{i-1,j}}{(\Delta y)^2}\right]$$

$$+ Du\left[\frac{\phi_{i+1,j} - 2\phi_{i,j} + \phi_{i-1,j}}{(\Delta y)^2}\right] \quad ...(18)$$

$$\left[\frac{\phi_{i,j+1} - \phi_{i,j}}{\Delta t}\right] + v_{i,j}\left[\frac{\phi_{i+1,j} - \phi_{i,j}}{\Delta y}\right] = \frac{1}{Sc}\left[\frac{\phi_{i+1,j} - 2\phi_{i,j} + \phi_{i-1,j}}{(\Delta y)^2}\right]$$

$$+ Sr\left[\frac{\theta_{i+1,j} - 2\theta_{i,j} + \theta_{i-1,j}}{(\Delta y)^2}\right] \quad ...(19)$$

3.0 Method of Solution

The governing Equations (11) to (14) are to be solved under the initial and boundary conditions of equation (15). The finite difference method is applied t o solve these equations.

The equivalent finite difference scheme of equations (11) to (14) are given by

A milling machine is a machine tool that removes metal as the work is fed against a rotating multipoint cutter.

The milling cutter rotates at high speed and it removes metal at a very fast rate with the help of multiple cutting edges.

Milling machine is used for machining flat surfaces, contoured surfaces, surfaces of revolution, external and internal threads, and helical surfaces of various cross- sections, etc.

In the work, up-mailing is used to remove the metal in the form of small chips by a rotating cutter against the direction of travel of the workpiece.

Fig 1: Face Milling Cutter

Fig 2: Operating on Milling Machine

Fig 3: Surface Roughness Measurement Instrument (Taylor Hobson Subtronics3+)

The Surtronic 3+ a portable is used for the measurement of surface texture and is suitable for use in both the workshop and laboratory.

Mild steel is used as a workmaterial, which is a common materialused in industry.Face milling cutter is used as tool with diameter (100mm),24 teeth, side (12.5mm) and arbor diameter 25mm.The milling machine model is **XW6032**

Table 1: The Process Parameters and their Levels

Process Parameter	Levels		
	1	2	3
Speed (m/min), V	565.48	724.92	1089.085
Feed rate (mm/min), f	20	32	45
Depth of cut (mm), d	0.5	0.75	1.00
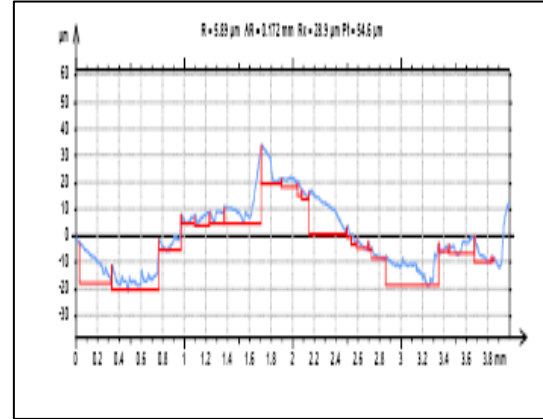
4.0 Analysis and Discussion
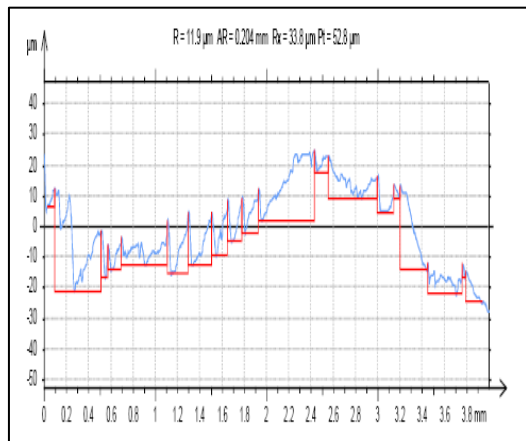
Fig 4: V=565.74m/min,F=20mm/min.,D=0.5mm

Fig 5: V=565.74m/min,F=32mm/min.,D=0.5mm

Fig 6: V=565.74m/min,F=45mm/min.,D=0.5mm
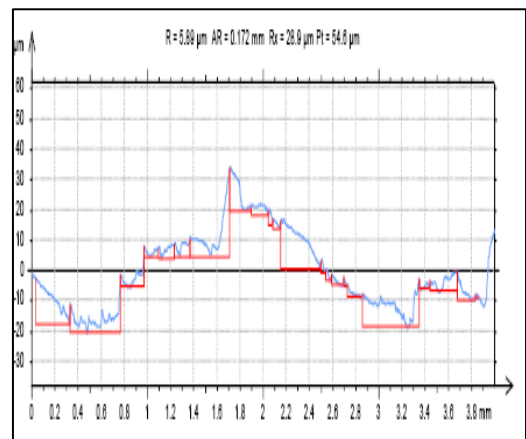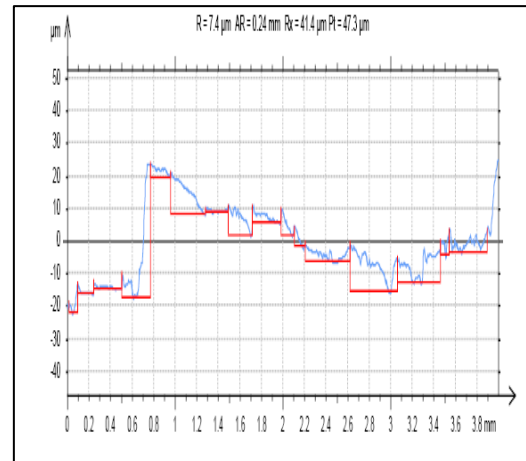

Fig 7: V=775.273m/min,F=20mm/min,D=0.5mm

Fig 8: V=775.273m/min,F=32mm/min.,D=0.5mm
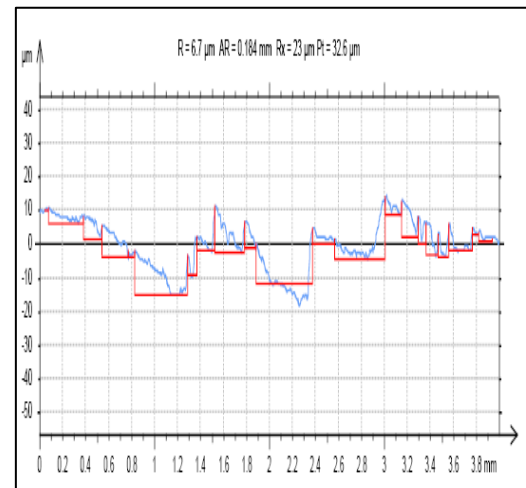
Fig 9: V=775.273m/min,F=45mm/min.,D=0.5mm

Fig 12:
V=1089.573m/min,F=45mm/min.,D=0.5mm
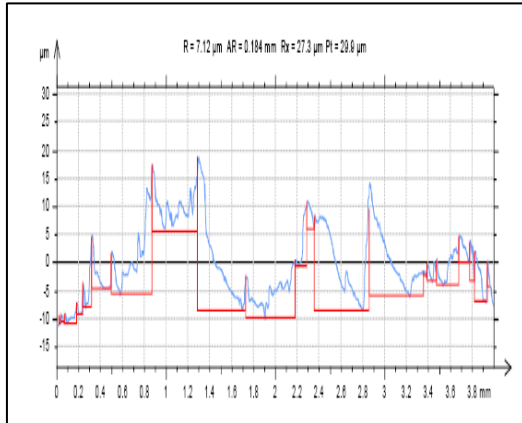
Fig 10:
V=1089.573m/min,F=20mm/min.,D=0.5mm

Fig 13: V=565.74 m/min,F=20mm/min.,D=0.75mm
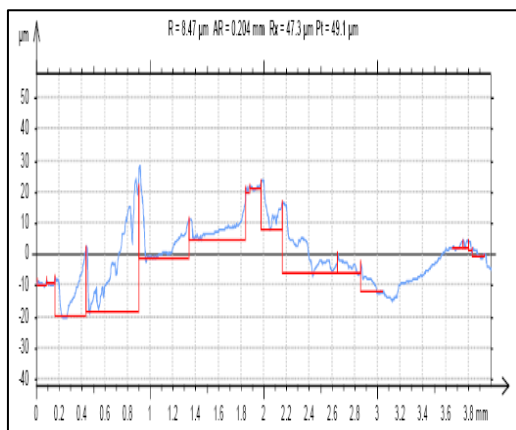
Fig 11:
V=1089.573m/min,F=32mm/min.,D=0.5mm
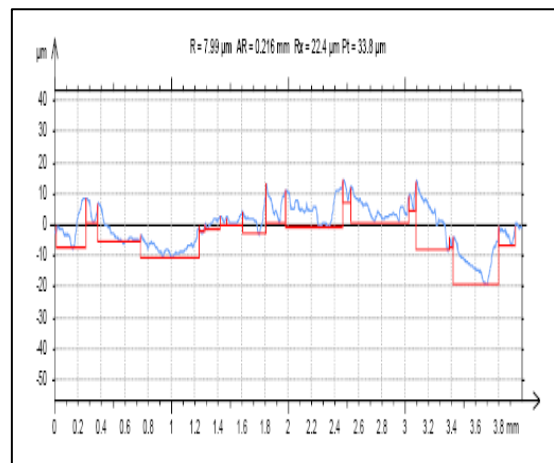
Fig 14: V=565.74m/min,F=32mm/min.,D=0.75mm
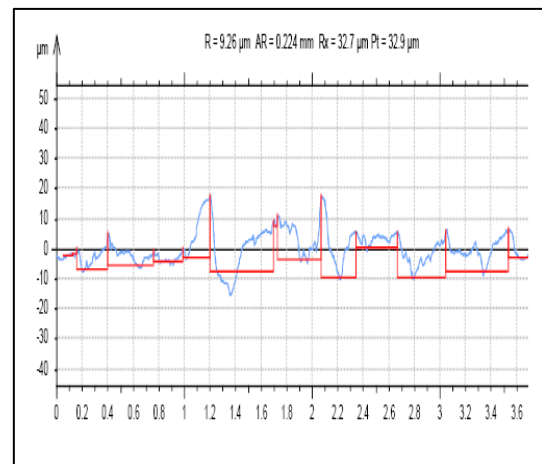
Fig 15: V=565.74m/min,F=45mm/min.,D=0.75mm
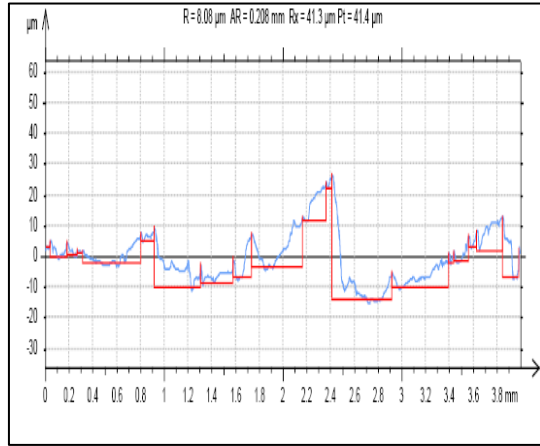
Fig 18: V=775.273m/min,F=45mm/min,D=0.75mm
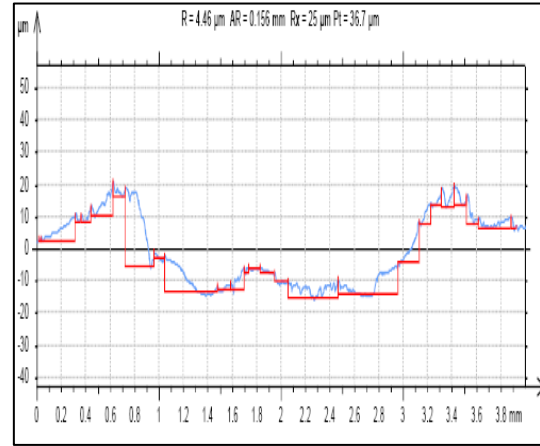
Fig 16: V=775.273m/min,F=20mm/min,D=0.75mm
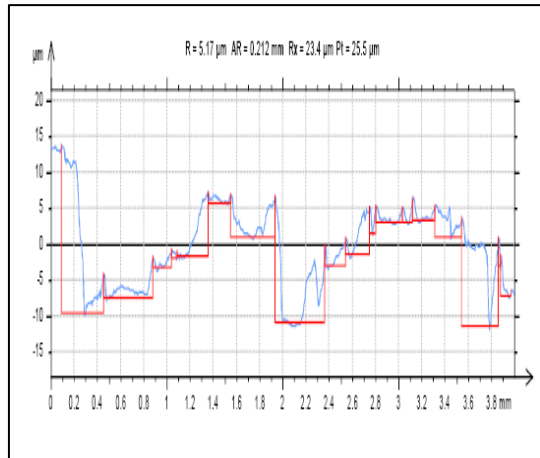
**Fig 19:
V=1089.573m/min,F=20mm/min.,D=0.75mm**
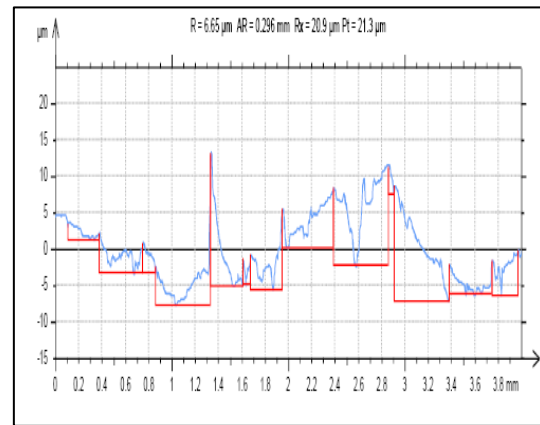
Fig 17: V=775.273m/min,F=32mm/min,D=0.75mm
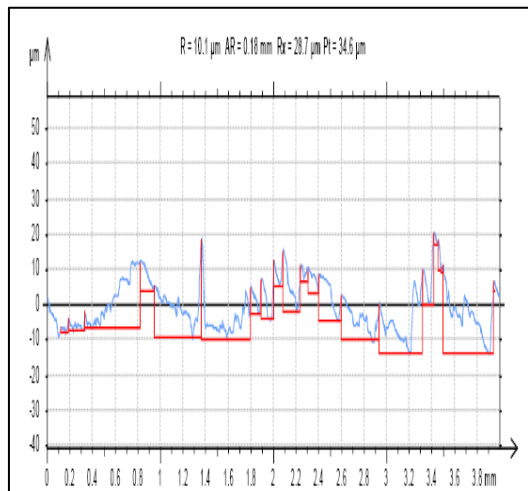
**Fig 20:
V=1089.573m/min,F=32mm/min.,D=0.75mm**
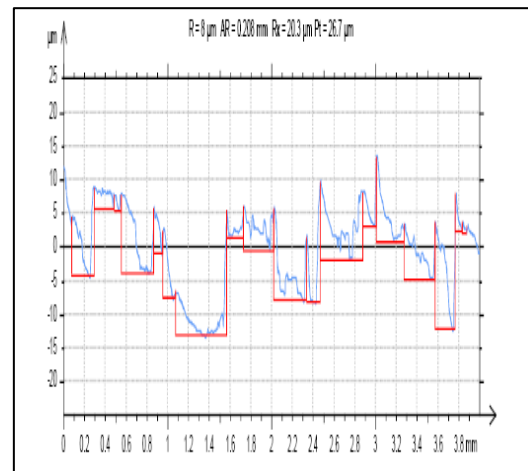
Fig 21:
V=1089.573m/min,F=45M/MIN.,D=0.75MM
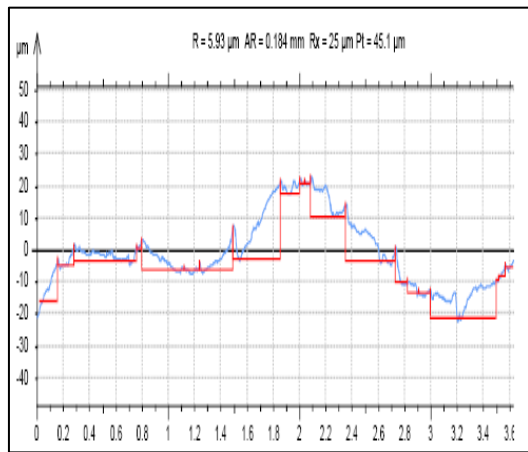
Fig 24: V=565.74m/min,F=45mm/min.,D=1.00mm
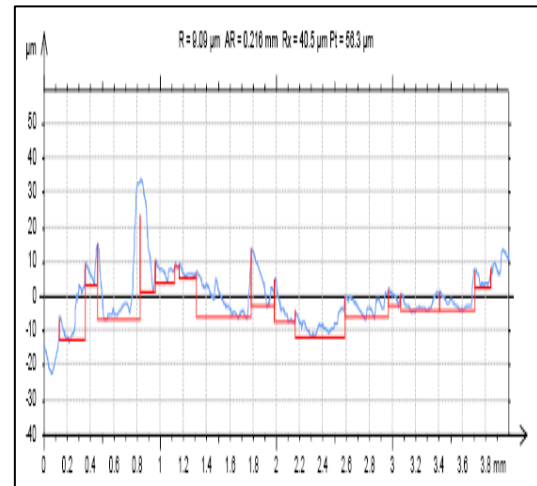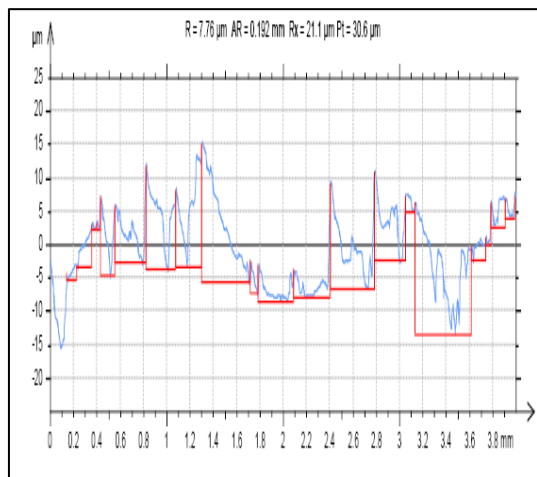

Fig 22: V=565.74m/min,F=20mm/min.,D=1.00mm

Fig 25:
V=775.273m/min,F=20mm/min.,D=1.00mm
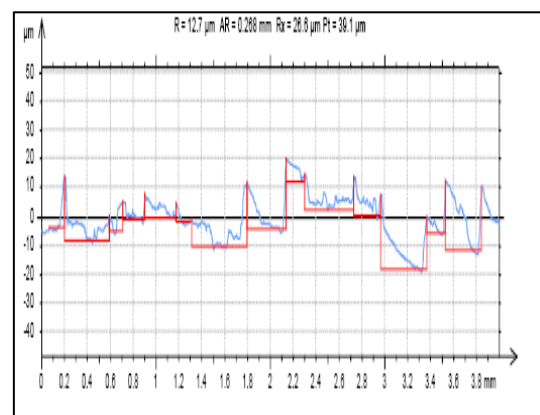
Fig 23: V=565.74m/min,F=32mm/min.,D=1.00mm

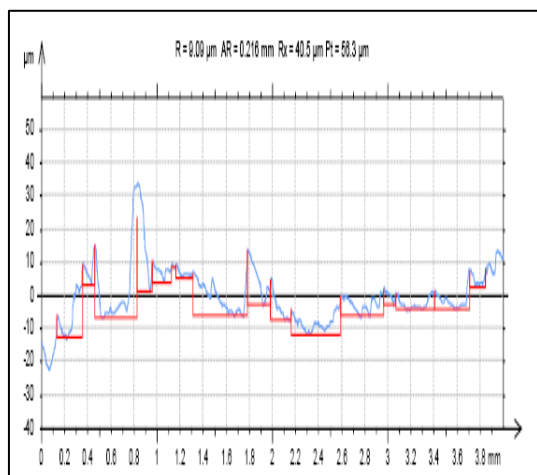

Fig 26:
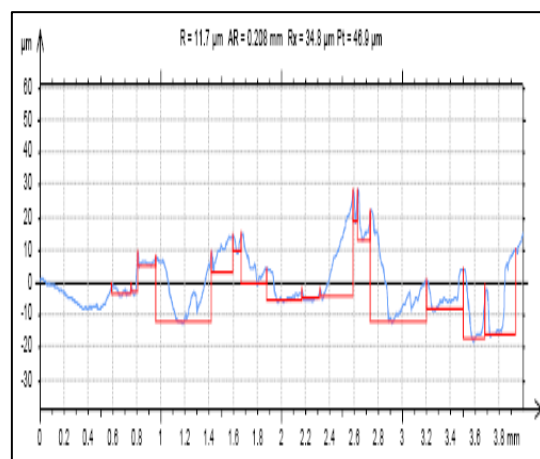**V=775.273m/min,F=32mm/min.,D=1.00mm**

Fig 27:
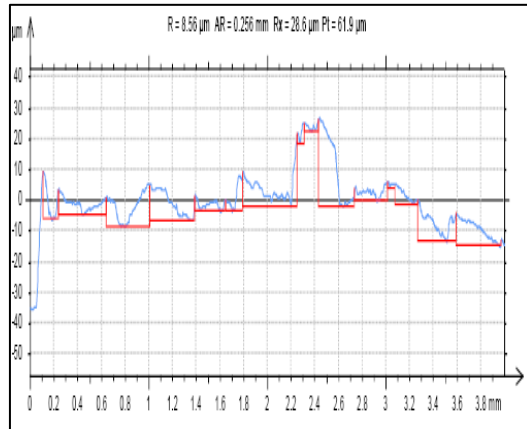**V=775.273m/min,F=45mm/min.,D=1.00mm**

Fig 28:
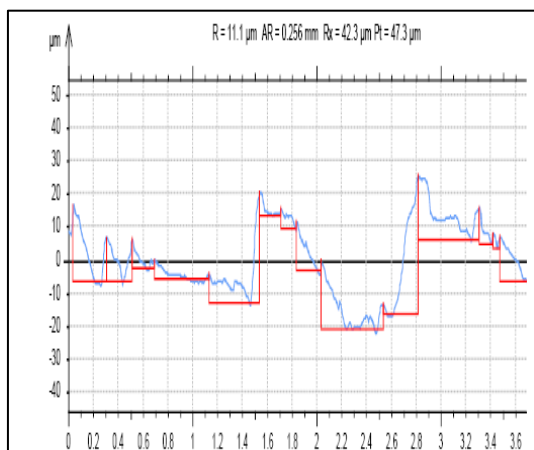**V=1089.573m/min,F=20mm/min.,D=1.00mm**

Fig 29:
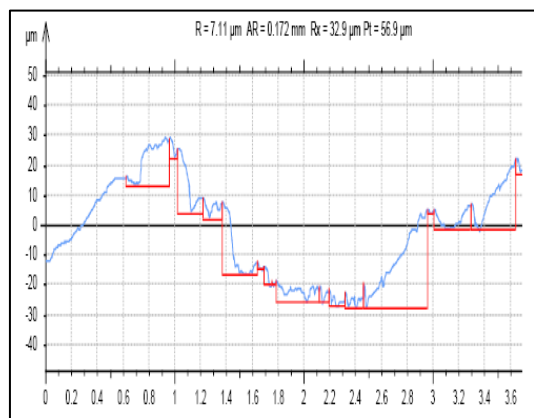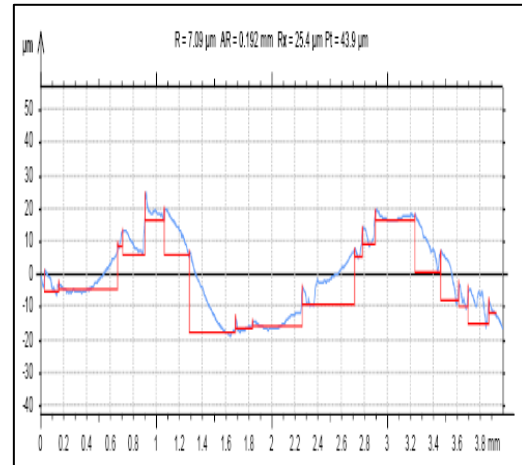**V=1089.573m/min,F=32mm/min.,D=1.00mm**

Fig 30:
V=1089.573m/min,F=45mm/min.,D=1.00mm

4.1 Roughness and waviness motifs (ISO 12085) for "R" parameters
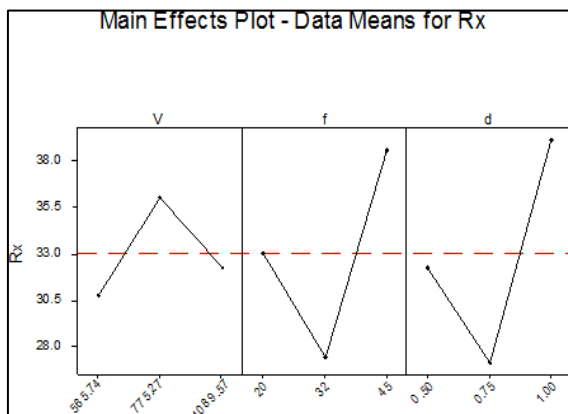
R (Average depth of roughness motifs) increase for cutting speed upto 775.27m/min and than decrease with increase in cutting speed. R decrease for feed up to 32mm/min. and then increase with increase in feed.R decrease for depth of cut up to 0.50 mm and then increase with increase in depth of cut.
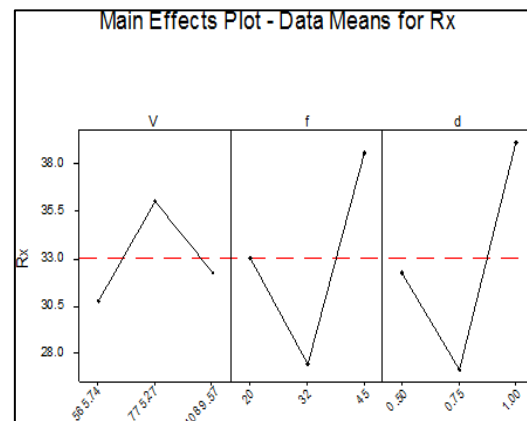
### 4.2 Roughness and waviness motifs (ISO 12085) for ―Arparameters

Ar (Average spacingof roughness motifs) increase for cutting speed upto 775.27m/min and than decrease with increase in cutting speed.

Ar decreasefor feed up to 32mm/min. and then increase with increase in feed. Ar increasesfor depth of cut up to 0.75 mm and then increase with increase in depth of cut.

Main Effects Plot - Data Means for Rx

4.3 Roughness and waviness motifs (ISO 12085) for "Rx" parameters

Rx (Maximum depth of roughness motifs) increase for cutting speed upto 775.27m/min and than decrease with increase in cutting speed. Rx decrease for feed up to 32mm/min. and then increase with increase in feed.R decrease for depth of cut up to 0.50 mm and then increase with increase in depth of cut.

Main Effects Plot - Data Means for Rx
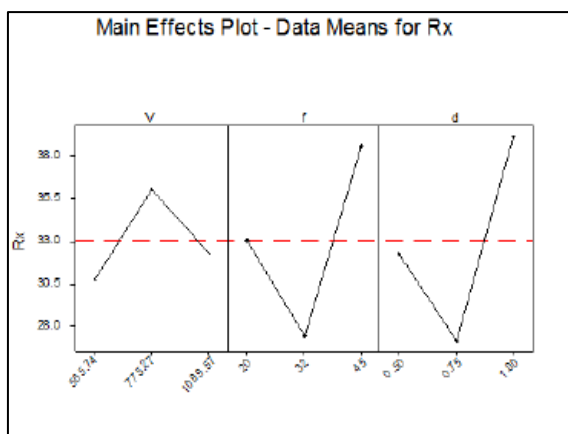
5.0 Conclusions

The conclusions drawn from the results and graphs display clearly that

a   Depth of cut is the significant factor. Optimum values of Rx are 775.27 m/min, 32mm/min and 0.75mm. Optimum values of Ar are 565.74 m/min, 32mm/rev and0 .50mm. Optimum values of R (roughness) are 565.74 m/min, 32mm/rev and 0.5mm.

b   The Feed rate is a significant factor. Optimum values of Ar are 775.27 m/min, 32mm/min and0 .50mm.

c   Feed rate and depth of cut are significant factor. Optimum values of Rx are 775.27m/min, 32mm/min and 0.75mm.

Nomenclature

Parameter Description
Ra Parameter of roughness
The MOTIF (R & W) parameters
R Average depth of roughness motifs
Rx Maximum depth of roughness motifs
Ar Average spacing of roughness motifs
Wx Maximum depth of waviness motifs
Rsm Average spacing of waviness motifs
Pt Maximum depth of the raw profile
The "Rk" family of parameters
Rk Depth of the roughness core profile
Rpk Top portion of the surface to be worn away
Rvk Lowest part of the surface retaining the lubricant
MR1 Upper limit of the core roughness
MR2 Lowest limit of the core roughness

References

[1]   Hasan Oktem, Tuncay Erzuruml, Fehmi Erzincanli**d** Prediction of minimum surface roughness in end milling mold parts using neural network and genetic algorithm, Materials and Design 27, 2006, 735–744.

[2]   Julie Z. Zhang, Joseph C. Chenb, E. Daniel Kirby, Surface roughness optimization in an end-milling operationusing the Taguchi design method, Journal of Materials Processing Technology 184 (2007) 233–239

[3]   Mohammed T. Hayajneh, Montasser S. Tahat, Joachim Bluhm A Study of the Effects of Machining Parameters on the SurfaceRoughness in the End-Milling Process © 2007 Jordan Journal of Mechanical and Industrial Engineering, Volume 1, Number 1, Sep. 2007 ISSN 1995-6665pp 1 – 5.

[4]   P.G. Benardos, G.C. VosniakosPrediction of surface roughness in CNC face milling using neuralnetworks and Taguchi's design of experiments, Robotics and Computer Integrated Manufacturing 18, 2002, 343–354

[5] Ranganath. M. S,Vipin, Lalit Kumar, Jitender Kumar Surface Texture Analysis in Turning of Mild Steel Using Carbide Inserts2014 International Journal of Advance Research and Innovation. 2, 3,2014, 601-606

[6] Vipin and H. Kumar, Surface Roughness Prediction Model by Design of Experiments for Turning Leaded Gun Metal, International Journal of Applied Engineering Research, 4, 12, 2009, 2621–2628.